

A Redox Non-Innocent Ligand Controls the Life Time of a Reactive Quartet Excited State - An MCSCF Study of $[\text{Ni}(\text{H})(\text{OH})]^+$

Yavuz Dede,[†] Xinhao Zhang,[‡] Maria Schlangen,[‡] Helmut Schwarz,^{*,‡} and Mu-Hyun Baik^{*,†}

Department of Chemistry and School of Informatics, Indiana University, Bloomington, Indiana 47405, and Institut für Chemie, Technische Universität Berlin, Straße des 17. Juni 135, DE-10623 Berlin, Germany

Received March 17, 2009; E-mail: Helmut.Schwarz@mail.chem.tu-berlin.de; mbaik@indiana.edu

Abstract: The electronic structures of the low and high-spin states of the cationic complex $[\text{Ni}(\text{H})(\text{OH})]^+$ that was previously found to be highly reactive toward CH_4 and O_2 were examined. Earlier computational work suggested that the low-spin doublet state D_0 of the $\text{Ni}^{\text{III}}-d^7$ system is significantly lower in energy than its high-spin quartet analogue Q_1 . Recent DFT-studies indicated, however, that Q_1 is the reactive species requiring Q_1 to have a sufficiently long lifetime for undergoing thermal reactions with the small molecule reactants under single collision conditions in the gas phase. These observations raise the question as to why Q_1 does not spontaneously undergo intersystem crossing. Our work based on DFT, coupled-cluster and MCSCF calculations suggests that the hydroxyl ligand behaves as a redox noninnocent ligand and becomes oxidized to formally afford an electronic structure that is consistent with a $\text{Ni}^{\text{II}}-(\text{OH})^\bullet$ species. As a result, the doublet and quartet ground states are not related by a single electron spin flip and the intersystem crossing becomes inhibited, as indicated by unexpectedly small spin-orbit coupling constants. After extensive sampling of the potential energy surfaces, we concluded that there is no direct way of converting Q_1 to the ground state doublet D_0 . Alternative multistep pathways for the $Q_1 \rightarrow D_0$ decay involving doublet excited states were also evaluated and found to be energetically not accessible under the experimental conditions.

Introduction

Small molecule activation is of prime importance in catalysis. Recently, we reported experimental^{1,2} and density functional theory (DFT) studies³ on $[\text{Ni}(\text{H})(\text{OH})]^+$, which under thermal condition activates CH_4 and O_2 . Both substrates are of tremendous interest as they have wide ranging technical applications and give rise to many intellectually challenging chemical transformations.⁴ Formally a $\text{Ni}^{\text{III}}-d^7$ ion, this molecule can adopt either a low-spin doublet (D_0) or a high-spin quartet (Q_1) state. Previously, Ugalde⁵ and co-workers found that D_0 is 19 kcal mol⁻¹ lower in energy than Q_1 at the B3LYP/DZVP level of theory. $[\text{Ni}(\text{H})(\text{OH})]^+$ in the D_0 state is believed to readily undergo reductive elimination to afford $[\text{Ni}(\text{OH}_2)]^+$, which is thermodynamically stable and, as shown experimentally,^{1,2} practically inert toward CH_4 and O_2 . We showed³ that the formation of most of the products can be explained using Q_1 as the reactive species, leading to the proposal that Q_1 is responsible for the observed chemistry. We must therefore assume that Q_1

has a finite lifetime in the gas phase to react, for example, with CH_4 or O_2 . Given the fact that the $Q_1 \rightarrow D_0$ transformation is computed to be highly exergonic, it is difficult to understand why intersystem crossing (ISC) does not take place spontaneously to simply deactivate the reactive Q_1 state first affording the D_0 state of $[\text{Ni}(\text{H})(\text{OH})]^+$, which will spontaneously form the chemically inert doublet state of $[\text{Ni}(\text{OH}_2)]^+$. Since single determinant methods such as DFT may be unreliable for estimating the relative energies of different spin states,⁶⁻¹¹ it is convenient to suspect a failure of DFT and speculate that Q_1 rather than D_0 is the ground state in reality. Because the species under investigation are transition metal (TM) compounds in either the doublet or quartet spin states, examination of the system is a challenging task and standard tools of computational chemistry are not fully adequate for understanding the related ISC phenomena, involving crossing of the potential energy

[†] Indiana University.

[‡] Technische Universität Berlin.

- (1) Schlangen, M.; Schroeder, D.; Schwarz, H. *Angew. Chem., Int. Ed.* **2007**, *46*, 1641–1644.
- (2) Schlangen, M.; Schwarz, H. *Helv. Chim. Acta* **2008**, *91*, 379–386.
- (3) Zhang, X.; Schlangen, M.; Dede, Y.; Baik, M.-H.; Schwarz, H. *Helv. Chim. Acta* **2009**, *92*, 151–164.
- (4) Arakawa, H. *Chem. Rev.* **2001**, *101*, 953–996.
- (5) Irigoras, A.; Elizalde, O.; Silanes, I.; Fowler, J. E.; Ugalde, J. M. *J. Am. Chem. Soc.* **2000**, *122*, 114–122.

- (6) Daku, L. M. L.; Vargas, A.; Hauser, A.; Fouqueau, A.; Casida, M. E. *ChemPhysChem* **2005**, *6*, 1393–1410.
- (7) Fouqueau, A.; Mer, S.; Casida, M. E.; Daku, L. M. L.; Hauser, A.; Mineva, T.; Neese, F. *J. Chem. Phys.* **2004**, *120*, 9473–9486.
- (8) Fouqueau, A.; Casida, M. E.; Daku, L. M. L.; Hauser, A.; Neese, F. *J. Chem. Phys.* **2005**, *122*, 044110–044113.
- (9) Ganzenmuller, G.; Berkaine, N.; Fouqueau, A.; Casida, M. E.; Reiher, M. *J. Chem. Phys.* **2005**, *122*, 234321–234312.
- (10) Reiher, M.; Salomon, O.; Hess, B. A. *Theor. Chem. Acc.* **2001**, *107*, 48–55.
- (11) Salomon, O.; Reiher, M.; Hess, B. A. *J. Chem. Phys.* **2002**, *117*, 4729–4737.

surfaces (PESs) and spin state changes. Multireference methods that are appropriate at least for a qualitatively correct description of the problem are technically demanding to conduct and difficult to interpret. In this work we employed electronic structure theory at DFT, coupled-cluster^{12–16} and CASSCF¹⁷ in combination with perturbative second order corrections (MRMP)¹⁸ levels to examine why Q_1 displays any finite lifetime at all and how it may decay to the D_0 state.

Computational and Technical Details

Multi configurational self-consistent field (MCSCF) calculations of the complete active space (CAS)¹⁹ type were performed to explore ground and low lying excited states (doublet and quartet spin symmetries) of the complex $[\text{Ni}(\text{H})(\text{OH})]^+$ as well as density functional theory (DFT) and coupled cluster calculations. Throughout the discussion, designation of the species is done with capital letters for the doublet (D) and quartet (Q) and subscripts are used to denote the ground (D_0) and excited (D_1) states. The computations mainly employed the 6-311+G(d,p)²⁰ and Dunning type correlation consistent cc-pVTZ all electron basis sets^{21,22} of triple- ζ quality. Both basis sets were recently reported²³ to show good performance for spin-state energetics of TM complexes. Results with other basis sets such as cc-pVQZ and aug-cc-pVTZ and Los Alamos effective core potentials, LACVP,^{24,25} used for comparisons were also reported. In order to properly include both dynamic and nondynamic correlation effects, perturbation corrections to the CASSCF calculations were done within the framework of Multi Configuration Quasi-Degenerate Perturbation Theory -to the second order- due to Nakano.¹⁸ The so-called *intruder states*²⁶ problem occasionally seen in the perturbation expansion of the reference CASSCF wave function due to very small or vanishing energy denominators were treated by utilizing an energy denominator shift of 0.02. Excited state MCSCF calculations²⁷ used the state averaged formalism with equal weights for all the states involved. The minimum energy crossing point (MECP) on the intersection seam of the Q_1 and D_0 surfaces was located with the method due to Farazdel and Dupuis²⁸ which is a gradient based constrained optimization technique and uses quasi-Newton schemes for the Hessian update, hence originally called Lagrange-Newton.²⁹ Seam optimization was done at CAS(11,11)/6-311+G(d,p), CAS(13,13)/cc-pVTZ, and OPBE/cc-pVTZ levels of theory. Manual corrections to the CAS(11,11)/6-311+G(d,p) optimized MECP were done by scanning the PES that connects it to Q_1 along the single dimension representing the

simultaneous transformations of all 6 internal coordinates.³⁰ This linear gradual coordinate transformation was also studied between D_0-Q_1 and D_1-Q_1 at CAS(11,11)/6-311+G(d,p) and CAS(13,13)/cc-pVTZ levels. These data were used to generate the Morse curve fits shown in Figure 1 (and in the SI) allowing the comparison of the structure and energetics of optimized CPs vs interpolated crossing regions. More details are given in the Supporting Information.

Nonadiabatic coupling of the PESs of different spin states at the CPs was studied by computing the spin-orbit coupling constants (SOCCs) using the full Pauli-Breit Hamiltonian,^{31–33} that includes both one electron and two electron terms at CAS(11,11)/6-311+G(d,p) and CAS(13,13)/cc-pVTZ levels. SOC calculations used nonorthogonal orbitals with the same fixed MCSCF core for both states and optimized the active orbitals. Although the initial states in the SOC calculations are configuration state functions (CSF) hence pure spin states, off-diagonal matrix elements were introduced to the Hamiltonian in the SOC calculations and the SOCCs reported are corresponding to the eigenvalues of the SO-Hamiltonian (H_{SO}), thus obtained after the diagonalization of H_{SO} . These initial states perturbed by inclusion of the SOC were still used to designate the SOCCs, for example, when referred to D_0-Q_1 SOCC, this is the matrix element of the H_{SO} between the two true spin states. In order to avoid vanishing of the SOC integrals, no use of symmetry was invoked in the SOC calculations, thus the only vanishing SOCCs were between two identical states due to hermiticity.³³ Also the effect of including excited CSFs to the H_{SO} (up to ten) from each multiplicity was carefully investigated and found not to significantly³⁴ affect the computed SOCCs. More than 10 lowest roots of the SO matrix were monitored in each SOC calculation. The matrix elements of the H_{SO} vanish for $\Delta S > 1$ but the effect of higher multiplicities in particular the sextets were investigated since they interact with quartets and thus doublets are indirectly affected through the intermediate quartets. The doublet-quartet SOCCs were only affected around one tenth of a cm^{-1} from this inclusion of sextets. More details about the construction of the method and the computer implementation are reported by Fedorov and Gordon³³ and Furlani and King.^{35,36}

DFT calculations employed the B3LYP^{37–43} and OPBE^{44,45} functionals. Coupled cluster geometry optimizations were done with inclusion of iterative single and double excitations (CCSD) and the energies reported throughout were obtained with inclusion of perturbative triples (CCSD(T)) on CCSD optimized geometries. Expectation value of the total spin operator, $\langle S^2 \rangle$ for DFT and

- (12) Pople, J. A.; Head-Gordon, M.; Raghavachari, K. *J. Chem. Phys.* **1987**, *87*, 5968–5975.
- (13) Cizek, J. *J. Chem. Phys.* **1966**, *45*, 4256–4266.
- (14) Cizek, J.; Paldus, J. *Int. J. Quantum Chem.* **1971**, *5*, 359–379.
- (15) Sinanoglu, O. *J. Chem. Phys.* **1962**, *36*, 706–717.
- (16) Purvis, G. D., III; Bartlett, R. J. *J. Chem. Phys.* **1982**, *76*, 1910–1918.
- (17) Roos, B. O. In *Advances In Chemical Physics*; Lawley, K. P., Ed.; Wiley & Sons: Chichester, 1987; Vol. 69, pp 399–445.
- (18) Nakano, H. *J. Chem. Phys.* **1993**, *99*, 7983–7992.
- (19) Also known as fully optimized reaction space (FORS).
- (20) Raghavachari, K.; Binkley, J. S.; Seeger, R.; Pople, J. A. *J. Chem. Phys.* **1980**, *72*, 650–654.
- (21) Dunning, T. H., Jr. *J. Chem. Phys.* **1989**, *90*, 1007–1023.
- (22) Balabanov, N. B.; Peterson, K. A. *J. Chem. Phys.* **2005**, *123*, 064107.
- (23) Güell, M.; Luis, J. M.; Sola, M.; Swart, M. *J. Phys. Chem. A* **2008**, *112*, 6384–6391.
- (24) Hay, P. J.; Wadt, W. R. *J. Chem. Phys.* **1985**, *82*, 270–283.
- (25) Hay, P. J.; Wadt, W. R. *J. Chem. Phys.* **1985**, *82*, 299–310.
- (26) Witek, H. A.; Choe, Y.-K.; Finley, J. P.; Hirao, K. *J. Comput. Chem.* **2002**, *23*, 957–965.
- (27) In this multi-state case, MP2 corrected CASSCF calculations are known as MCQDPT2.
- (28) Farazdel, A.; Dupuis, M. *J. Comput. Chem.* **1991**, *12*, 276–282.
- (29) Fletcher, R. In *Practical Methods of Optimization*; John Wiley & Sons: New York, 1987.

- (30) This was performed because the numerical errors at the optimized seam turned out to yield differences more than 0.01 kcal/mol between the two states.
- (31) Lefebvre-Brion, H.; Field, R. W. In *Perturbations in the Spectra of Diatomic Molecules*; Academic Press Inc.: New York, 1986; pp 28–134.
- (32) Bethe, H. A.; Salpeter, E. E. In *Quantum Mechanics of One- and Two-Electron Atoms*; Springer Verlag: Berlin, 1957; pp 170–205.
- (33) Fedorov, D. G.; Gordon, M. S. *J. Chem. Phys.* **2000**, *112*, 5611–5623.
- (34) The difference was less than one inverse cm.
- (35) Harry, F.; King, T. R. *J. Comput. Chem.* **1988**, *9*, 771–778.
- (36) Furlani, T. R.; King, H. F. *J. Chem. Phys.* **1985**, *82*, 5577–5583.
- (37) Becke, A. D. *Phys. Rev. A* **1988**, *38*, 3098–3100.
- (38) Becke, A. D. *J. Chem. Phys.* **1993**, *98*, 5648–5652.
- (39) Lee, C. T.; Yang, W. T.; Parr, R. G. *Phys. Rev. B* **1988**, *37*, 785–789.
- (40) Slater, J. C. *Quantum Theory of Molecules and Solids, Vol. 4: The Self-Consistent Field for Molecules and Solids*; McGraw-Hill: New York, 1974.
- (41) Vosko, S. H.; Wilk, L.; Nusair, M. *Can. J. Phys.* **1980**, *58*, 1200–1211.
- (42) Stephens, P. J.; Devlin, F. J.; Chabalowski, C. F.; Frisch, M. J. *J. Phys. Chem.* **1994**, *98*, 11623–11627.
- (43) Hertwig, R. H.; Koch, W. *Chem. Phys. Lett.* **1997**, *268*, 345–351.
- (44) Handy, N. C.; Cohen, A. J. *Mol. Phys.* **2001**, *99*, 403–412.
- (45) Perdew, J. P.; Burke, K.; Ernzerhof, M. *Phys. Rev. Lett.* **1997**, *78*, 1396–1396.

coupled cluster calculations was monitored for potential problems due to possible deficiencies in the single reference approach. T1 diagnostic for the coupled cluster calculations was monitored as well.

Vibrational analyses were performed at the same level with the geometry optimizations and used to confirm the species to be true minima with no imaginary frequencies. Unscaled harmonic frequencies were employed to obtain the zero-point vibrational energy (ZPVE) and entropy corrections. No restrictions on symmetry were imposed. Unless otherwise stated relative energies (in kcal mol⁻¹) reported throughout are in reference to the ground state low-spin doublet species D₀.

The GAMESS (versions = 24 MAR 2007 (R6) and 11 APR 2008 (R1)) program suite⁴⁶ was used for MCSCF and most of the DFT calculations. Some DFT calculations were performed with the Jaguar 7.0 program.⁴⁷ Coupled cluster calculations were carried out with the Gaussian⁴⁸ package.

Design of the Active Space. Active spaces (electrons, orbitals) studied, started from the smallest possible (3,4) including only four of the 3d orbitals of Ni. Most of such small active spaces which did not include the ligand based orbitals yielded unusual geometries for both states and failed to give a description that parallels the DFT and CCSD results. Among the ill behaving active spaces a 15,10 AS that includes all the Ni 3d electrons and orbitals without any 4d orbitals was found to be inappropriate. A 15,13 AS including the full set of Ni 3d but three Ni 4d orbitals suffers from intruder states at the MP2 corrected level although it appeared balanced at the CAS level. Furthermore, with active spaces smaller than 11,11 the molecular orbital optimization procedure did not preserve the same active orbitals for the two states, which must be avoided in order to generate self-consistent properties. We surmised that it is not plausible to consider an active space only with Ni electrons and orbitals, because neglecting the participation of the hydroxide and hydride electrons may prove to be a severe oversimplification and predetermine the role of these ligands in the chemistry that the [Ni(H)(OH)]⁺ complex exhibits. The most important ASs utilized were the 11,11; 15,13; and 13,13. Our discussions are mainly based on the results from CAS(11,11)/6-311+G(d,p) and CAS(13,13)/cc-pVTZ calculations.

The 11 electrons in 11 orbitals active space was comprised of the three highest lying 3d and three 4d orbitals of Ni, the three 2p orbitals of oxygen, and the 1s orbital of both hydrogens. At the dissociation limit of the ligands this 11,11 CAS should transform into a CAS(3,6) for Ni³⁺, CAS(6,4) for OH⁻ and CAS(2,1) for H⁻.⁴⁹ In preliminary studies, inclusion of the 4d set proved to be crucial as a consequence of the well-known double shell effect in transition metals⁵⁰ because we have a 3d set which is more than half filled. Although the 11,11 AS was carefully built placing two of the 3d orbitals that were always doubly occupied in the reference wave function to the MCSCF core, one must consider that this protocol may not be appropriate as not all of the 3d set experience the explicit correlation treatment and this asymmetry may lead to erroneous results. Therefore, we compared a few of these calculations against the other MCSCF results and we found that while the absolute energies and geometrical parameters change somewhat, the core chemical picture presented in this work remained unaltered. The 13,13 AS did not exclude any Ni 3d electrons and two shells were used for all electrons. In this AS the low lying σ bonding

orbital generated from the 1s orbital of hydroxyl hydrogen and O-2p along the O-H bond axis (2p(y)) was kept in the MCSCF core for computational feasibility.

A 15,15 active space built from the full set of Ni 3d and 3d' orbitals which also included the same ligand valence orbitals as in 11,11 AS was also tested. This envisioned 15,15 active space had more than 16 million CSFs for each spin symmetry. Although the size of the CI matrix diagonalization problem that can be dealt with increases rapidly with the advances in high performance parallel computing, the current limit of feasible calculations is generally thought to be reached with a few million CSFs or ~14 active orbitals.⁵¹ After much experimentation, we concluded that a 15,15 AS is not feasible with currently available computational resources.

To examine the uniformity of the CAS, in particular for CAS(11,11), CAS(15,13) and CAS(13,13) calculations, natural orbitals (NO) were carefully analyzed for all the species discussed. NOs diagonalize the one electron density matrix with nonintegral diagonal elements from 0 to 2 being the occupation numbers (NOON), and they are a convenient way of building the MCSCF wave function as they provide the shortest CI expansion possible. NOONs and orbital isosurface plots were used to eliminate solutions with undesired orbital rotations. The diffuseness of the bases and the canonicalization of the orbitals resulted in a slight mixing of the MCSCF optimized orbitals, but a careful inspection of the NOs revealed that the 1s and 2s orbitals of O, and the 1s, 2s, 3s, and the 2p and 3p sets of Ni were clearly excluded from the CAS and were always kept as the lowest 11 orbitals of the CASSCF core. Conservation of the active orbitals for each case was also carefully checked.

Discussion

Structural and Thermochemical Features. Our calculations at various levels of theory suggest that the ground state geometries of the two spin states display significant differences and they are energetically well separated. The geometries and relative energies together with the $\langle S^2 \rangle$ values as a measure for the spin contamination, for the doublet (D₀) and quartet (Q₁) ground states are shown in Table 1.

The low-spin D₀ state is associated with a more compact structure having a Ni-O bond length of ~1.7 Å at all levels of theory. The Ni-O bond is notably longer in Q₁ with all coupled-cluster and CASSCF treatments affording bond lengths around 2.0 Å. Surprisingly, the Ni-O bond length of Q₁ decreases with increasing basis set size within DFT and the difference with respect to D₀ is much less pronounced compared to the CCSD and CASSCF results. It is interesting to note that this feature of Q₁ showing a significantly longer Ni-O bond length is present at the B3LYP/LACVP/6-31G** level of theory. Our previous benchmarks^{52,53} show B3LYP/LACVP/6-31G** results to be reasonably reliable for transition metal complexes. Its good performance among a set of effective core potentials was also recently²³ confirmed, but it is unresolved here whether the aforementioned decrease in the Ni-O bond length for the high-spin state is unrealistic and if there is an overestimation of the bonding with DFT employing large basis sets for this particular case.⁵⁴ CASSCF calculations can be expected to give a more localized picture and hence result in a pronounced elongation for the Ni-O bond length but this feature is also captured with

(46) Schmidt, M. W.; Baldridge, K. K.; Boatz, J. A.; Elbert, S. T.; Gordon, M. S.; Jensen, J. H.; Koseki, S.; Matsunaga, N.; Nguyen, K. A.; Su, S.; Windus, T. L.; Dupuis, M.; Montgomery Jr, J. A. *J. Comput. Chem.* **1993**, *14*, 1347-1363.

(47) *Jaguar 7.0*; Schrödinger, LLC: New York, 2007.

(48) Frisch, M. J.; et al. *Gaussian03, Revision C.02*; Gaussian Inc.: Wallingford, CT: 2004.

(49) Note that a 2,1 active space by itself is meaningless and it is given here for a better description of the 11,11 CAS used in the study.

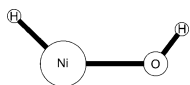
(50) Pierloot, K. In *Computational Organometallic Chemistry*; Cundari, T. R., Ed.; Marcel Dekker Inc.: New York, 2001; pp 123-130.

(51) Neese, F.; Petrenko, T.; Ganyushin, D.; Olbrich, G. *Coord. Chem. Rev.* **2007**, *251*, 288-327.

(52) Baik, M.-H.; Friesner, R. A. *J. Phys. Chem. A* **2002**, *106*, 7407-7415.

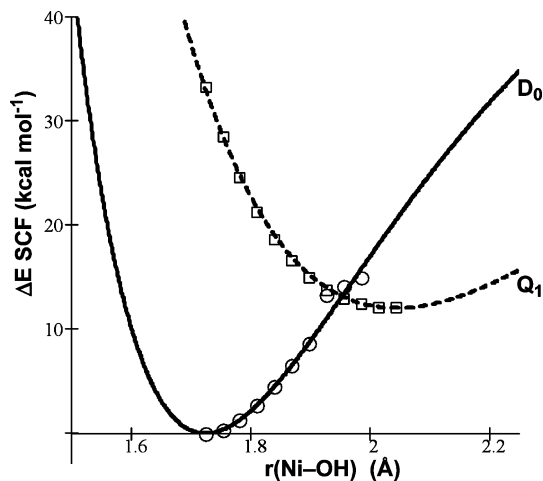
(53) Many studies from our own work have proven LACVP** basis to give reliable results for geometrical parameters of transition metal complexes.

(54) We will address this issue in detail as a separate study.

Table 1. Selected Geometrical Parameters^a (Å and deg), Spin Contamination, and Relative Energy Difference (kcal mol⁻¹) of the D₀ and Q₁ States of $[\text{Ni}(\text{H})(\text{OH})]^+$


model chemistry		r(H–Ni)	r(Ni–O)	r(O–H)	$\varphi(\text{HNiO})$	$\varphi(\text{NiOH})$	$\theta(\text{HNiOH})$	$\langle S^2 \rangle$	$\Delta E(\text{SCF})$
B3LYP/LACVP/6-31G**	D ₀	1.428	1.690	0.977	85.2	123.4	−3.2	0.79	
	Q ₁	1.489	1.945	0.988	119.0	125.2	−0.3	3.76	19.6
B3LYP/6-311+G(d,p)	D ₀	1.433	1.685	0.977	86.2	122.5	0.0	0.79	
	Q ₁	1.558	1.730	0.978	148.4	128.8	0.0	3.76	20.0
B3LYP/cc-pVTZ	D ₀	1.437	1.677	0.974	86.8	123.9	0.1	0.79	
	Q ₁	1.564	1.720	0.976	146.3	129.0	0.1	3.76	19.6
B3LYP/aug-cc-pVTZ	D ₀	1.438	1.679	0.975	86.7	124.1	0.0	0.79	
	Q ₁	1.565	1.719	0.976	146.6	129.2	0.1	3.76	19.6
B3LYP/cc-pVQZ	D ₀	1.438	1.678	0.973	86.7	124.2	0.0	0.79	
	Q ₁	1.565	1.718	0.975	146.8	129.5	0.0	3.76	19.6
OPBE/6-311+G(d,p)	D ₀	1.440	1.683	0.976	87.3	125.2	0.0	0.76	
	Q ₁	1.558	1.730	0.978	148.4	128.8	0.0	3.75	22.1
OPBE/cc-pVTZ	D ₀	1.429	1.678	0.977	85.3	121.0	0.1	0.76	
	Q ₁	1.553	1.721	0.978	146.1	124.7	0.0	3.75	21.4
CCSD(T)/6-311+G(d,p)	D ₀	1.438	1.680	0.969	85.3	124.9	−0.2	0.77	17.3
	Q ₁	1.489	2.015	0.980	122.2	126.5	−0.1	3.75	24.5 ^b
CCSD(T)/cc-pVTZ	D ₀	1.427	1.674	0.967	81.3	124.6	−0.1	0.78	25.3
	Q ₁	1.488	1.992	0.979	122.2	124.6	0.0	3.78	26.6 ^c
CAS(11,11)/6-311+G(d,p)	D ₀	1.509	1.762	0.975	86.6	120.7	34.9	n/a	16.8
	Q ₁	1.573	2.123	0.985	143.6	129.1	−0.1	n/a	25.9 ^d
CAS(15,13)/6-311+G(d,p)	D ₀	1.464	1.704	0.976	81.7	124.3	0.0	n/a	20.7
	Q ₁	1.554	2.096	0.985	135.7	127.1	−0.3	n/a	34.7 ^d
CAS(13,13)/cc-pVTZ	D ₀	1.446	1.723	0.953	86.5	124.5	0.2	n/a	12.0
	Q ₁	1.502	2.043	0.960	128.2	131.1	0.1	n/a	35.8 ^d

^a CCSD(T) calculations used CCSD optimized geometries. MRMP calculations used CAS optimized geometries. ^b CCSD(T)/6-311++G(3d,2p)//CCSD/6-311+G(d,p). ^c CCSD(T)/aug-cc-pVTZ//CCSD/cc-pVTZ. ^d MRMP corrected.

**Figure 1.** Potential energy surfaces of the lowest doublet and quartet states at CAS(13,13)/cc-pVTZ level. Only one coordinate $r(\text{Ni}-\text{O})$ is shown on the x axis.

the CCSD calculations. Other important geometrical features showing the compactness of D₀ relative to Q₁ are the notably shorter H–Ni bond length and smaller HNiO bond angle reproduced at all the levels of theory. Energetically, our calculations give preference of the D₀ over the Q₁ state by 20 to 30 kcal mol⁻¹. Having significant geometrical differences B3LYP/LACVP/6-31G** and B3LYP/cc-pVQZ energy splittings surprisingly coincide at 19.6 kcal mol⁻¹ and all DFT predictions gather around 20 kcal mol⁻¹. The highest level CCSD(T) energy splitting calculated at CCSD(T)/aug-cc-pVTZ//CCSD/cc-pVTZ level being 26.6 kcal mol⁻¹ is very close to the 24.5 kcal mol⁻¹ from the CCSD(T)/6-311++G(3d,2p)//CCSD/6-311+G(d,p) treatment. The CCSD(T) prediction also

matches well with MRMP(11,11) values that quantify the energy splitting to be 25.9 kcal mol⁻¹, whereas MRMP(15,13) and MRMP(13,13) energy differences are both greater than 30 kcal mol⁻¹. In summary, we found some notable variance of structure and the associated energies at different levels of theory, but a clear general trend can be recognized from all these calculations with some confidence. Inclusion of ZPVEs lower the energy separation by 1.9 to 2 kcal mol⁻¹ at all levels and the CCSD(T)/aug-cc-pVTZ energy splitting becomes 24.6 kcal mol⁻¹. We conclude that the energy splitting between the low and high-spin states of $[\text{Ni}(\text{H})(\text{OH})]^+$ is ca. 25 kcal mol⁻¹ in clear preference of the D₀ state. These results do not support the speculation that DFT may fail to properly describe the energetic ordering of the two states. Our work provides strong support for the conclusion that D₀ is indeed lower in energy than Q₁. The multireference treatments also lend support to the results from the single-determinant methods as inspection of the CASSCF wave functions at all the levels considered indicate both Q₁ and D₀ to be dominated by a single configuration. Taken together, we conclude that D₀ is the ground state of the $[\text{Ni}(\text{H})(\text{OH})]^+$ complex and that the significant thermodynamic driving force for the Q₁→D₀ transformation identified previously by Ugalde et al.⁵ is realistic and perhaps even higher by ca. 5 kcal mol⁻¹. Thus, ISC should be feasible thermodynamically. Key to understanding the finite lifetime of the Q₁ state must therefore lie in the kinetics of the transformation which requires understanding the ISC at a reasonable level of theory. Unfortunately, standard quantum chemical methods do not allow for studying ISC, which is intrinsically a dynamic problem, without invoking severe approximations. As a first step, we can examine whether or not the potential energy surfaces (PESs) of the two states treated independently from each other will cross. The

Table 2. Selected Geometrical Parameters^a (Å and deg), and Relative Energies with Respect to Q₁ (kcal mol⁻¹) of the Q₁-D₀ CP of [Ni(H)(OH)]⁺

model chemistry		r(H-Ni)	r(Ni-O)	r(O-H)	φ(HNiO)	φ(NiOH)	θ(HNiOH)	ΔE(SCF)
OPBE/cc-pVTZ	Q ₁ -D ₀	1.537	1.726	0.979	136.1	123.6	0.7	0.5
CAS(11,11)/6-311+G(d,p)	Q ₁ -D ₀	1.576	2.118	0.985	135.3	129.5	23.2	0.3 ^a
CAS(13,13)/cc-pVTZ	Q ₁ -D ₀	1.503	2.000	0.959	110.3	128.4	0.0	1.1 ^a

^a MRMP corrected energy differences are 0.1 kcal mol⁻¹ and 2.6 kcal mol⁻¹ respectively.

crossing point can then be assumed to be analogous^{28,55-57} to the transition state in the standard model^{58,59} and allow for estimating the energetic penalty for reaching the crossing point.

Minimum Energy Crossing Points of D₀-Q₁ and D₁-Q₁ Surfaces. Identifying crossing points between two PESs is challenging from both technical and conceptual perspectives.⁶⁰ Convergence is often difficult and depending on the topology of the PESs, severe changes in the electronic structures of the involved states may be expected upon small structural changes. Properties of the CP are expected to be coupled with the extent of interaction of the wave functions. Thus, understanding ISC is by no means a routine process. The standard multireference treatment of the crossing region employed here does not go beyond the clamped nuclei formalism for the optimization of the seam and a quantum dynamics study that is technically more challenging at the moment may be more appropriate⁶¹ as this is a region where nuclear motion becomes important. Fortunately, our detailed analysis provides a general chemical insight and qualitative understanding capturing what we believe to be the most important features of this interesting system.

Figure 1 illustrates the shape of the two PESs along the vector connecting D₀ and Q₁ equilibrium geometries. One scenario that would explain the kinetic protection of Q₁ from ISC is that the CP is energetically inaccessible high. Our calculations indicate, however, that there is a crossing point close to Q₁ both geometrically and energetically (Figure 1). Both the interpolated crossing region and the optimized crossing point do not have high energy barriers. Relative to Q₁ the optimized CP is 0.5 kcal mol⁻¹ and 1.1 kcal mol⁻¹ higher at the OPBE/cc-pVTZ and CAS(13,13)/cc-pVTZ levels respectively.⁶² Interestingly, the CP showed significant multireference character for the doublet state. At the CAS(13,13)/cc-pVTZ level the dominant determinants of the MCSCF wave functions have CI coefficients of 0.98 and 0.06 for the quartet and 0.80, 0.46, 0.28, 0.14, and 0.14 for the doublet state. The corresponding CI coefficients at the CAS(11,11)/6-311+G(d,p) level are 0.97 and 0.12 for the quartet and 0.66, 0.54, 0.38, 0.19, and 0.19 for the doublet state. These indicate that multireference methods are important for the analysis of the CP. The geometrical parameters and relative energies of the CP located at different levels are reported in Table 2. CP and Q₁ always show small differences which are energetically tolerable indicating the flatness of the PES in the vicinity of Q₁.

The energetic and structural similarity of CP to Q₁ equilibrium suggests that the hypothesis of energy-based kinetic protection of Q₁ is unlikely to be correct. Moreover, a classical interpretation of the dynamics at this crossing is in favor of ISC since Q₁ may sample the region with high frequency as the structural parameters are close and there is not a large energetic penalty for reaching the crossing. Thus, both the transition state energies and the overall thermodynamics suggest that rapid ISC followed by facile reductive elimination to afford the kinetically inert [Ni(OH₂)]⁺ species should be possible, in stark contrast to the experimental observations.

The second requirement for a successful surface hopping is that there is significant coupling between the two states. Thus, we investigated the extent of the nonadiabatic coupling in this formally spin-forbidden process. As the overall spin momentum is not conserved ISCs have to be promoted by spin-orbit coupling, where the orbital angular momentum can absorb the momentum change associated with the spin flip. Transition metal centers are particularly effective in facilitating ISC because they commonly display relatively large SOC as a result of the high nuclear charge. The spin-orbit coupling constant can be computed using the Pauli-Breit spin-orbit coupling operator (eq 1)

$$\hat{H}_{\text{SO}} = \frac{\Omega^2}{2} \left\{ \sum_{i=1}^{N_{\text{el}}} \sum_{\alpha=1}^{N_{\text{atoms}}} \frac{Z_{\alpha}}{|\vec{r}_j - \vec{r}_{\alpha}|^3} [(\vec{r}_i - \vec{r}_{\alpha}) \times \vec{p}_i] \cdot \vec{s}_i - \sum_{i=1}^{N_{\text{el}}} \sum_{j \neq i}^{N_{\text{el}}} \frac{1}{|\vec{r}_i - \vec{r}_j|^3} [(\vec{r}_i - \vec{r}_{\alpha}) \times \vec{p}_i] \cdot [\vec{s}_i + 2\vec{s}_j] \right\} \quad (1)$$

where Ω is the fine structure constant, α the nuclear and i and j the electron coordinates, respectively, Z_{α} the nuclear charge, p_i the electron momentum, and s_i the electron spin operators.³¹⁻³³ The one electron SO operator given by the first double sum is more important than the two electron SO operator given by the second double sum as the former grows much more rapidly and is usually an order of magnitude larger.³³ Following the works of Furlani and King³² and Fedorov and Gordon³⁵ the matrix element $\langle {}^{2S+1}\Psi_i | \hat{H}_{\text{SO}} | {}^{2S'+1}\Psi_j \rangle$ is defined as the SOCC. Inspecting the SO operator, we can easily understand why transition metal centers often display a large SOCC and are therefore effective in promoting ISC as the nuclear charge of transition metals is high and the electrons in the d -orbitals are contracted when compared to the s - and p -analogues.

The computed SOCC can be benchmarked by analyzing the spin-mixed state splittings that are induced by SOC in bare atoms where the spectroscopic fine structure is experimentally available. These energy splittings range from a few tens to a few hundreds of cm⁻¹ in light nonmetals and reach thousands of cm⁻¹ for the late first row TMs, going up to approximately 10000 cm⁻¹ in heavy metal atoms.⁶³ In molecules it is difficult

(55) Ragazos, I. N.; Robb, M. A.; Bernardi, F.; Olivucci, M. *Chem. Phys. Lett.* **1992**, *197*, 217-223.

(56) Robb, M. A.; Bernardi, F.; Olivucci, M. *Pure Appl. Chem.* **1995**, *67*, 783-789.

(57) Nguyen, K. A.; Gordon, M. S.; John, A.; Montgomery, J.; Michels, H. H.; Yarkony, D. R. *J. Chem. Phys.* **1993**, *98*, 3845-3849.

(58) Eyring, H. *J. Chem. Phys.* **1935**, *3*, 107-115.

(59) Laidler, K. J.; King, M. C. *J. Phys. Chem.* **1983**, *87*, 2657-2664.

(60) Harvey, J. N. *Phys. Chem. Chem. Phys.* **2007**, *9*, 331-343.

(61) Tully, J. C. *Faraday Discuss.* **1998**, *110*, 407-419.

(62) At CAS(11,11)/6-311+G(d,p) level the CP is practically isoenergetic with Q₁ with its energy being only 0.3 and 0.1 kcal mol⁻¹ above Q₁ at CAS and MRMP levels, respectively.

(63) Fedorov, D. G.; Koseki, S.; Schmidt, M. W.; Gordon, M. S. *Int. Rev. Phys. Chem.* **2003**, *22*, 551-592.

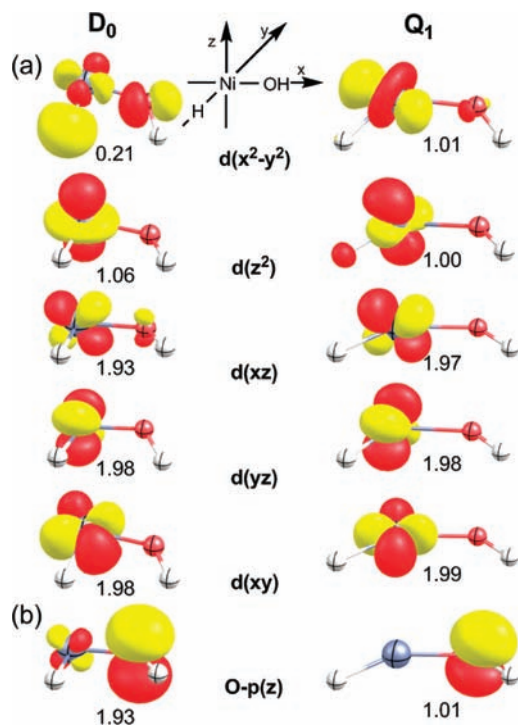


Figure 2. Isosurface plots (isodensity value = 0.075 a.u.) and occupation numbers of the most important natural orbitals, for the D_0 and Q_1 states of $[\text{Ni}(\text{H})(\text{OH})]^+$ at CAS(13,13)/cc-pVTZ level. See Supporting Information for the very similar NOs obtained at other MCSCF levels.

to estimate the quality of computed SOCCs because reliable experimental data is much more scarce, but they are expected to follow the trends seen for atomic calculations. In a previous study for a doublet-quartet transition of a Ti complex, a SOCC of $\sim 50 \text{ cm}^{-1}$ was judged to be small since a TM would normally be expected to generate larger SOC.⁶⁴ On the other hand, different studies reported relatively small SOCCs at a few cm^{-1} to facilitate ISC.^{60,65} Given the variations in the magnitude of the computed numbers, their dependence on the level of theory and the formulation of the H_{SO} used, there is no obvious scale that can be used to determine whether a certain SOCC value can be considered sufficient to allow for ISC to occur or not. Consequently when interpreting SOCCs one should not forget the source of the molecular SOC as being atomic in nature and judge them as large or small with this distinction taken into account.

We computed the SOCC of the Q_1 and D_0 states at the crossing point and found it to be 16.8 and 8.0 cm^{-1} at the CAS(11,11)/6-311+G(d,p) and CAS(13,13)/cc-pVTZ levels, respectively.⁶⁶ These values are surprisingly low and provide a first hint that the ISC may be prohibited primarily for an electronic reason. The key to understanding the unexpectedly low SOCC lies in the electronic structure of the two spin states. The effect of electronic structure mismatch on the magnitude of SOCC was discussed previously in detail by Danovich and Shaik⁶⁷ where the computed SOCCs were smaller than the

Table 3. Mulliken Atomic Spin Densities for the Ni and O Atoms in the D_0 and Q_1 States of $[\text{Ni}(\text{H})(\text{OH})]^+$

model chemistry	D_0		Q_1	
	$\rho_{\text{Mull}}(\text{Ni})$	$\rho_{\text{Mull}}(\text{O})$	$\rho_{\text{Mull}}(\text{Ni})$	$\rho_{\text{Mull}}(\text{O})$
B3LYP/LACVP/6-31G**	0.90	0.23	1.69	1.04
B3LYP/6-311+G(d,p)	0.90	0.23	1.87	0.74
B3LYP/cc-pVTZ	0.92	0.20	1.87	0.72
B3LYP/aug-cc-pVTZ	0.93	0.19	1.86	0.72
B3LYP/cc-pVQZ	0.93	0.20	1.89	0.70
OPBE/6-311+G(d,p)	0.68	0.40	1.89	0.80
OPBE/cc-pVTZ	0.70	0.38	1.87	0.78
CCSD(T)/6-311+G(d,p)	0.86	0.06	2.06	1.10
CCSD(T)/cc-pVTZ	0.85	0.06	2.07	1.07

expected in case of iron, in spite of its high atomic constant. To derive a similar level of understanding, we conducted a full scale molecular orbital analysis of the two spin states.

The D_0 state is a low-spin $\text{Ni}^{\text{III}}-d^7$ complex and is therefore expected to display three doubly occupied frontier MOs and one singly occupied MO, whereas Q_1 is the high-spin analogue and should show two doubly occupied and three singly occupied frontier orbitals. Thus, D_0 should exhibit a spin density of ~ 1 centered on Ni, whereas ~ 3 should be seen for Q_1 . Computed spin densities for D_0 approximately show the expected values of 0.93 and 0.85 at the B3LYP and CCSD levels, respectively (Table 3). The spin density distribution of the Q_1 , however, is inconsistent with a classical high-spin $\text{Ni}^{\text{III}}-d^7$ system. Instead of the expected three unpaired electrons centered on Ni, only two unpaired electrons are found. The third electron is localized on the oxygen atom according to both DFT and coupled cluster calculations as indicated by spin densities of 1.89 and 2.07 on nickel and 0.70 and 1.07 on oxygen, respectively. A plausible interpretation of this finding is that the electronic structure of Q_1 is more consistent with a $\text{Ni}^{\text{II}}-(\text{OH})^\bullet$ species instead of the formally resonant $\text{Ni}^{\text{III}}-(\text{OH}^-)$ system that we expected initially. The high-spin Q_1 system can be envisioned to undergo an intramolecular redox reaction formally moving one electron from the hydroxy-moiety to the high-spin $\text{Ni}^{\text{III}}-d^7$ center to afford a $\text{Ni}^{\text{II}}-(\text{OH})^\bullet$ moiety. Although the geometrical parameters and relative energies of the low-spin and high-spin states show variation at the theoretical levels utilized, the electronic structure of Q_1 bearing an unpaired electron confined to oxygen is quite consistent in all calculations. This electronic structure mismatch between the D_0 and Q_1 provides a rationale for the kinetic protection of the quartet state against facile and efficient ISC, as the second criterion for effective ISC is not met, and quantified by the low SOCC and also conceptually verified by the analysis of the spin densities. The effect of this electronic structure mismatch on the magnitude of the SOCC is well understood once H_{SO} is inspected. Because of the $Z_\alpha (r_j - r_\alpha)^{-3}$ dependence of H_{SO} discussed above, spin orbit coupling has a highly localized nature. In reformulating the rules for SOCs in biradicals after the pioneering work of Salem and Rowland,⁶⁸ Michl⁶⁹ studied SO integrals involving orbitals that are not centered on the same atom and argued that that they can be neglected due to the r^{-3} dependence. The “short sighted” nature of SOC is a well documented phenomenon.^{70–72} We propose that the same effect is operational in the nickel complex and

(64) Moc, J.; Fedorov, D. G.; Gordon, M. S. *J. Chem. Phys.* **2000**, *112*, 10247–10258.

(65) Woeller, M.; Grimme, S.; Peyermhoff, S. D.; Danovich, D.; Filatov, M.; Shaik, S. *J. Phys. Chem. A* **2000**, *104*, 5366–5373.

(66) SOCCs computed two points beyond the crossing region on the interpolated reaction coordinate gives even lower values at a few inverse cm.

(67) Danovich, D.; Shaik, S. *J. Am. Chem. Soc.* **1997**, *119*, 1773–1786.

(68) Salem, L.; Rowland, C. *Angew. Chem., Int. Ed.* **1972**, *11*, 92–111.

(69) Michl, J. *J. Am. Chem. Soc.* **1996**, *118*, 3568–3579.

(70) McClure, D. S. *J. Chem. Phys.* **1949**, *17*, 905–913.

(71) Neese, F. *J. Chem. Phys.* **2003**, *118*, 3939–3948.

(72) Ballhausen, C. J. *Introduction to Ligand Field Theory*; MacGraw Hill: New York, 1962.

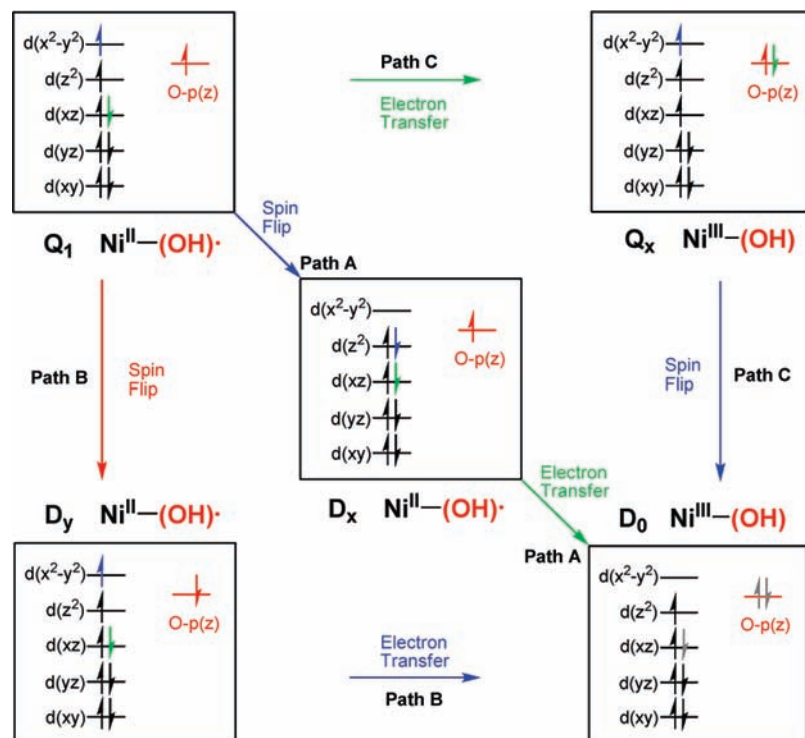


Figure 3. Schematic illustration of the required electronic structure changes for the $Q_1 \rightarrow D_0$ transformation.

the delocalized spin distribution of Q_1 is the primary reason for the inhibition of an otherwise plausible ISC.

Since the localization of one unpaired α electron to oxygen is exclusively responsible for the interesting properties of Q_1 we envisioned that this feature of the quartet should not be present in $[\text{Ni}(\text{H})(\text{H})]^+$. We carried out MCSCF calculations on this system and found that the two lowest lying doublet and quartet states which are analogous to D_0 and Q_1 for $[\text{Ni}(\text{H})(\text{OH})]^+$ show the anticipated high nonadiabatic coupling for a TM complex.⁷³ The SOCC was computed to be 397.4 cm^{-1} at the optimized CP and the confinement of a single electron on one of the H atoms was not present, highlighting the role of the radicaloid OH in $[\text{Ni}(\text{H})(\text{OH})]^+$ for the unexpectedly low SOCC and the related kinetic behavior.

Molecular Orbital Analysis of D_0 and Q_1 . To further verify the assignment of the formal oxidation states III and II to the Ni center in D_0 and Q_1 , respectively, and to better understand the electronic structure of Q_1 we analyzed the CASSCF natural orbitals (NOs). As mentioned above, our CASSCF calculations indicate that both wave functions are highly dominated by a single configuration with the formal representations at all the MCSCF levels

$$D_0: {}^2\Psi_{\text{MCSCF}} \approx 0.9[\text{closed shell}](d_z^2)(\alpha) + \sum_i c_i \Phi_i$$

$$Q_1: {}^4\Psi_{\text{MCSCF}} \approx 0.9[\text{closed shell}](d_z^2)(\alpha)(d_{x^2-y^2})(\alpha)O - pz(\alpha) + \sum_i c_i \Phi_i$$

where Φ_i are less important determinants. The five d -orbital dominated NOs of the D_0 and Q_1 states and their respective occupation numbers are shown in Figure 2a. There are three

doubly filled NOs of $d(xy)$, $d(yz)$, $d(xz)$ characters in D_0 . The $d(z^2)$ orbital is singly occupied, while $d(x^2-y^2)$ can be assigned to be empty for all practical purposes. Our calculations assign occupation numbers ranging from 0.20 to 0.25 to this NO originating from minor excited configurations in the multireference description of the doublet.⁷⁴ This orbital occupation pattern is fully consistent with what one expects for a low-spin d^7 -system. Interestingly, Q_1 shows three doubly occupied NOs that are $d(xy)$, $d(yz)$, $d(xz)$ dominated and two $d(z^2)$ and $d(x^2-y^2)$ based MOs that are singly occupied (Figure 2a). Thus, there are eight valence electrons at the Ni-center and the MO-diagram is that of a high-spin $\text{Ni}^{\text{II}}-d^8$ system. The third unpaired electron of this quartet state resides in the oxygen- $p(z)$ orbital, as shown in Figure 2b.⁷⁵ The corresponding oxygen orbital in the D_0 state is doubly occupied. This electronic structure is interesting for two main reasons:

(i) It provides a plausible explanation for why Q_1 does not readily undergo the $Q_1 \rightarrow D_0$ transformation: A simple spin flip does not take Q_1 to D_0 , but to an excited doublet state D_x , a low-spin $\text{Ni}^{\text{II}}(\text{OH})\bullet$ system (Path A in Figure 3). To reach D_0 , this state must execute a metal-to-ligand electron transfer thereby formally oxidizing the metal and reducing the ligand. Alternatively, another excited doublet D_y can be generated by the spin inversion of the odd electron residing on oxygen- $p(z)$ orbital. (Path B in Figure 3) This path will be less likely, however, as it requires the oxygen nucleus to promote spin inversion rather than Ni (*vide infra*). After reaching D_y the spin-allowed transition to D_0 can be achieved by a metal-to-ligand electron transfer. A third possibility is that Q_1 could undergo electron transfer first (Path C in Figure 3) to give an excited quartet state Q_x , the high-spin $\text{Ni}^{\text{III}}(\text{OH})\bullet$ state anticipated initially for Q_1 , from which D_0 can be reached by electron spin inversion.

(ii) The formulation of Q_1 as $\text{Ni}^{\text{II}}(\text{OH})\bullet$ offers an intuitive rationale for the unusual chemical reactivity of this ion in its thermal reaction with CH_4 and O_2 .^{1,2} Recently, there has been

(73) Dede Y.; Baik M.-H. To be published.

an increased awareness of the redox noninnocence of ligands,^{76–88} where a transition-metal center can intramolecularly oxidize ligands to give for example radicaloid M-oxyl species that can promote remarkable reactions.⁸⁹ We propose that the hydroxide group in $[\text{Ni}(\text{H})(\text{OH})]^+$ is a redox noninnocent ligand and that this feature is ultimately responsible for both the protection of Q_1 toward ISC and the rich gas-phase chemistry of this ion.

Having rationalized that the direct conversion $Q_1 \rightarrow D_0$ is inhibited because of incompatibility of the two electronic states, we must ask why the alternative pathways involving various excited states outlined above are not feasible. To answer this question, we explored the excited states of both the quartet and doublet spin states targeting the states similar to D_x , D_y and Q_x at the CAS(11,11) level of theory. Whereas these calculations proved challenging and were encountered by convergence problems, we were nonetheless able to locate and characterize the lowest excited states to a sufficient extent to extract some useful insights. It is important to recognize that excited states commonly display significantly higher levels of multireference character. Whereas the actual excited states are multideterminant representations, all of which are kept orthogonal to the ground state MCSCF wave function, the excited state representations above correspond to single configurations, each of which may be expected to significantly contribute to the state of interest. Therefore the conceptual single-determinant representations utilized in our discussion above may be deceptive in that they present an oversimplified picture. Thus our discussions of the excited state computations must be considered only semiquantitative in nature.

Our explorations indicate that there are many low lying doublet and quartet excited states involving mostly Ni-3d excitations. This is not surprising for a transition metal complex where there are a number of near-degenerate states due to close lying metal d-orbitals. As an approximation to the idealized D_y state the fourth excited doublet state at ~ 60 kcal mol⁻¹ is the lowest that developed significant β electron density on O- $p(z)$. Similarly, the fourth quartet excited state that is also approximately ~ 60 kcal mol⁻¹ higher in energy than the doublet ground state D_0 was the lowest excited state that showed

significant increase in natural orbital occupation of the O- $p(z)$ of 1.4 confirming that quartet states such as [closed shell] $d(xz)(\alpha)d(z^2)(\alpha)d(x^2-y^2)(\alpha)O-p(z)^2$ lie at relatively high energies.

From the conceptual approach illustrated in Figure 3 it is clear that those states involving spin inversion of the oxygen-based electron or double occupation of the oxygen-based orbital must be accessed if the pathways B or C are operative. Each of these can be excluded on the basis of their energy requirements. Realistically, only the first excited states are relevant and we found that D_1 , the first doublet excited state, is particularly interesting. Energetically, it lies halfway between the doublet and quartet ground states D_0 and Q_1 . D_1 is located at 8.7 kcal mol⁻¹ and 6.4 kcal mol⁻¹ at the CAS(11,11)/6-311+G(d,p) and CAS(13,13)/cc-pVTZ levels respectively therefore it lies 8.2 kcal mol⁻¹ and 6.6 kcal mol⁻¹ lower in energy than Q_1 . It is also physically sensible to focus on D_1 since Q_n can be expected to have rapid decay to Q_1 and D_n to D_0 in a spin allowed fashion.

A more detailed examination of the D_1 state reveals that the dominating determinant with a CI-coefficient of ~ 0.8 at both levels is the $\text{Ni}^{\text{II}}(\text{OH})\cdot$ excited state that we have labeled as D_x in Figure 3 (See Supporting Information for details). Thus, the $D_0 \rightarrow D_1$ excitation can be interpreted as mostly being a ligand-to-metal charge transfer in character that transforms the $\text{Ni}^{\text{III}}(\text{OH}^-)$ moiety into the $\text{Ni}^{\text{II}}(\text{OH})\cdot$ system. Therefore, the sequence of transformations $Q_1 \rightarrow D_1 \rightarrow D_0$ represents what we labeled as Path A in Figure 3. In an effort to identify a possible crossing point between the PESs of the Q_1 and D_1 states, we scanned the PESs along the vector connecting Q_1 and D_1 and were able to estimate a crossing point for the Q_1 and D_1 potential energy surfaces. We estimate the energy of this crossing point, CP¹ to be 5.5 and 3.9 kcal mol⁻¹ higher than Q_1 at the CAS(11,11)/6-311+G(d,p) and CAS(13,13)/cc-pVTZ levels respectively. The respective SOCC computed at the CP¹ are 416.7 cm⁻¹ and 411.9 cm⁻¹ demonstrating that spin-orbit coupling constants that are more in the expected range can be obtained between properly compatible states in the $[\text{Ni}(\text{H})(\text{OH})]^+$ complex. The notably larger SOCC is easy to understand because the $Q_1 \rightarrow D_1$ transformation involves spin inversion and slight reorganization of MOs that are all Ni-3d based, as illustrated in Figure 3. In spite of the strong coupling of Q_1 - D_1 states this pathway is unfeasible under the experimental conditions because the crossing point lies significantly higher in energy than the Q_1 state. Under the isolated conditions in the gas phase we do not expect Q_1 to recruit enough energy from its environment to reach the $Q_1 \rightarrow D_1$ crossing point.⁹⁰

Once all the information up to this point is collected, one wonders how these translate into actual physical quantities that can be measured, i.e. is there a prediction about the lifetime of Q_1 . To partly address this complex issue we carried out rate calculations with the nonadiabatic version of Rice-Ramsperger-Kassel-Marcus (RRKM) theory.⁹¹ The analytical expressions for the probabilities of surface hopping were studied by Nikitin,^{92,93} Delos and Thorson,⁹⁴ and Lorquet

(74) We do not claim ~ 0.2 to be a small occupation number but it simplifies the interpretation of the molecular orbital analysis performed.

(75) The alpha electrons avoiding each other are in part responsible for the longer Ni-O bond length of the high-spin state.

(76) Chaudhuri, P.; Verani, C. N.; Bill, E.; Bothe, E.; Weyhermuller, T.; Wieghardt, K. *J. Am. Chem. Soc.* **2001**, *123*, 2213–2223.

(77) Kaim, W.; Wanner, M.; Knodler, A.; Zalis, S. *Inorg. Chim. Acta* **2002**, *337*, 163–172.

(78) Ward, M. D.; McCleverty, J. A. *Dalton Trans.* **2002**, 275–288.

(79) Baik, M. H.; Newcomb, M.; Friesner, R. A.; Lippard, S. *J. Chem. Rev.* **2003**, *103*, 2385–2419.

(80) Yang, X.; Baik, M.-H. *J. Am. Chem. Soc.* **2006**, *128*, 7476–7485.

(81) Ray, K.; Petrenko, T.; Wieghardt, K.; Neese, F. *Dalton Trans.* **2007**, 1552–1566.

(82) Kirchner, B.; Wennmohs, F.; Ye, S.; Neese, F. *Curr. Opin. Chem. Biol.* **2007**, *11*, 134–141.

(83) Ringenberg, M. R.; Kokatam, S. L.; Heiden, Z. M.; Rauchfuss, T. B. *J. Am. Chem. Soc.* **2008**, *130*, 788–789.

(84) Lu, C. C.; DeBeer George, S.; Weyhermuller, T.; Bill, E.; Bothe, E.; Wieghardt, K. *Angew. Chem., Int. Ed.* **2008**, *47*, 6384–6387.

(85) Ketterer, N. A.; Fan, H.; Blackmore, K. J.; Yang, X.; Ziller, J. W.; Baik, M.-H.; Heyduk, A. F. *J. Am. Chem. Soc.* **2008**, *130*, 4364–4374.

(86) Storr, T.; Verma, P.; Pratt, R. C.; Wasinger, E. C.; Shimazaki, Y.; Stack, T. D. P. *J. Am. Chem. Soc.* **2008**, *130*, 15448–15459.

(87) Lu, C. C.; Bill, E.; Weyhermuller, T.; Bothe, E.; Wieghardt, K. *J. Am. Chem. Soc.* **2008**, *130*, 3181–3197.

(88) Muckerman, J. T.; Polyansky, D. E.; Wada, T.; Tanaka, K.; Fujita, E. *Inorg. Chem.* **2008**, *47*, 1787–1802.

(89) Yang, X.; Baik, M.-H. *J. Am. Chem. Soc.* **2008**, *130*, 16231–16240.

(90) Also note that SOCCs computed between higher quartet and doublet excited states at the two crossing points were never as much as Q_1 - D_1 SOCC.

(91) Forst, W. *Unimolecular Reactions A Concise Introduction*; Cambridge University Press: Cambridge, 2003.

(92) Nikitin, E. E. In *Advances in Quantum Chemistry, Volume 5*; Löwdin, P.-O., Ed.; Academic Press: New York, 1970; Vol. 5, pp 135–184.

(93) Nikitin, E. E. *Theory of Elementary Atomic and Molecular Processes in Gases*; Clarendon Press: London, 1974; Vol. 5, p 135–184.

(94) Delos, J. B.; Thorson, W. R. *Phys. Rev. A* **1972**, *6*, 728–745.

and co-workers.^{95–97} Although the applications^{98–102} generally proved to be useful, many uncertainties about the dynamics of the system should caution us about the quality of the numbers generated. There are rate calculations for ISCs reported in the literature which predicted highly different results for the experimentally determined life times.^{103,104} This is mainly due to the lack of information about the actual dynamics of the systems and quantitative reliability is questionable.⁹¹ More sophisticated quantum dynamics simulations that may become available in the future may provide a more appropriate treatment of this problem.¹⁰⁵

Nonetheless, we have computed the rate of ISC within the limits of currently available theories. Following the definitions of Forst⁹¹ the double-passage Landau–Zener (LZ)^{106,107}

$$p_{LZ}(\varepsilon_t) = 2 \left\{ 1 - \exp \left[\frac{-\Pi\beta}{4\varepsilon^{1/2}} \right] \right\} \quad (2)$$

transition probability for ISC given by eq 2 will vanish for energies below the crossing point and will not predict surface hopping in such occasions like ours. The nonadiabatic transition probability with the Airy function¹⁰⁸ (A_i) to approximate the overlap of vibrational wave functions and include tunneling effects is given as

$$p(\varepsilon_t) = \Pi^2 \beta^{4/3} A_i^2(-\varepsilon\beta^{2/3}) \quad (3)$$

where the dimensionless variables β , ε , and ε_0 are defined as:

$$\beta = \frac{4H_{12}^{3/2}}{\hbar} \left(\frac{\mu}{F\Delta F} \right)^{1/2} \varepsilon = (\varepsilon_t - E_c)\varepsilon_0 \varepsilon_0 = \frac{\Delta F}{2FH_{12}}$$

and the slopes F_1 and F_2 of the two PESs at the crossing define $\Delta F = |F_1 - F_2|$ and $F = |F_1 F_2|^{1/2}$. Here H_{12} is the SOCC, E_c is the energy of the crossing, μ the reduced mass of the system as it passes the crossing and ε_i is the initial energy of the molecule.

Using the probabilities of ISC (Table 4) as a pre-exponential factor and computing the rate of $Q_1 \rightarrow D_0$ transformation, a lifetime close to microseconds can be estimated for Q_1 at room temperature for a surface hopping barrier (E_a) of 1.1 kcal mol⁻¹.

Table 4. Calculated Probabilities, $p(\varepsilon_t)$ for ISCs and the Associated Half Lives for Q_1

ISC	$p(\varepsilon_t)$	E_a (kcal mol ⁻¹)	$t_{1/2}$ (sec)
$Q_1 \rightarrow D_0$	2.8×10^{-6}	1.1	2.6×10^{-7}
$Q_1 \rightarrow D_0$	7.7×10^{-13}	2.6	1.2×10^1
$Q_1 \rightarrow D_1$	1.8×10^{-17}	3.9	5.3×10^6

The path to D_1 is essentially blocked in spite of the large SOCC mainly due to CP¹ lying a few kcal mol⁻¹ above Q_1 . Probabilities for the $Q_1 \rightarrow D_1$ transformation are calculated to be less than 10^{-15} , thereby inhibiting the ISC and suggesting that the $Q_1 \rightarrow D_1$ ISC is energetically prohibitive. Using the surface hopping barrier calculated at MRMP(13,13)/cc-pVTZ level the probability for $Q_1 \rightarrow D_0$ transformation even goes below 10^{-12} which yields a lifetime of a few seconds for Q_1 thereby supporting the electronically forbidden nature of the $Q_1 \rightarrow D_0$ transformation. It is important to note that the presence of a TM in the molecule contributes to downsizing the ISC probability as it decreases the tunneling and affects the vibration along the Ni–O mode which is one important component of the quartet doublet transformation. In spite of the expected low accuracy of the computed rates due to the many intrinsic approximations, they provide support for the idea that D_1 is inaccessible from Q_1 and that Q_1 will likely exhibit a sufficiently long lifetime under the experimental condition to undergo reactions with CH₄ and/or O₂.

Conclusion

In conclusion, we propose that Q_1 displays a sufficiently long lifetime to allow for it undergoing various chemical reactions with small molecule substrates, because its electronic structure is incompatible with the lower energy configuration D_0 . This incompatibility is based on a redox noninnocent ligand OH, which becomes formally oxidized to afford an electronic structure that is better described as Ni^{II}-(OH)• instead of the more classical description of a Ni^{III}-(OH⁻) moiety. A simple spin inversion promoted by spin orbit coupling does not take the quartet Ni^{II}-(OH)• high-spin species to the low-spin analogue D_0 , which is a classical low-spin Ni^{III}-(OH⁻) complex ion. We found that a more viable pathway for ISC from electronic standpoint involves a two-step mechanism invoking the first doublet excited state D_1 , which is mostly the low-spin version of the Ni^{II}-(OH)• ion. We estimate the lowest energy crossing point between the Q_1 and D_1 surfaces to be 4 to 5 kcal mol⁻¹ higher than the energy of the quartet ground state Q_1 , which prevents it being reached with a reasonable rate under the gas phase experimental conditions.

Acknowledgment. We thank the NSF (CHE-0645381 to M.-H.B. and 0116050 to Indiana University), the Sloan Foundation, the Research Corporation, the Fonds der Chemischen Industrie, and the DFG (Cluster of Excellence “Unifying Concepts in Catalysis” at TU Berlin) for financial support. The Scientific and Technological Research Council of Turkey (TÜBİTAK) and the Alexander von Humboldt Stiftung are acknowledged for postdoctoral fellowships to Y.D. and X.Z., respectively. Fruitful discussions with Prof. Srinivasan S. Iyengar are gratefully acknowledged.

Supporting Information Available: Computational details, additional discussion, Cartesian coordinates, energy components of all structures and complete ref 4 and 48. This material is available free of charge via the Internet at <http://pubs.acs.org>.

JA902093F

- (95) Desouter-Lecomte, M.; Lorquet, J. C. *J. Chem. Phys.* **1979**, *71*, 4391–4403.
- (96) Lorquet, A. J.; Lorquet, J. C.; Forst, W. *Chem. Phys.* **1980**, *51*, 253–260.
- (97) Lorquet, J. C.; Leyh-Nihant, B. *J. Phys. Chem.* **1988**, *92*, 4778–4783.
- (98) Delos, J. B. *J. Chem. Phys.* **1973**, *59*, 2365–2369.
- (99) Lorquet, A. J.; Lorquet, J. C.; Forst, W. *Chem. Phys.* **1980**, *51*, 261–270.
- (100) Harvey, J. N.; Aschi, M. *Faraday Discuss.* **2003**, *124*, 129–143.
- (101) Schröder, D.; Heinemann, C.; Schwarz, H.; Harvey, J. N.; Dua, S.; Blanksby, S. J.; Bowie, J. H. *Chem.—Eur. J.* **1998**, *4*, 2550–2557.
- (102) Cui, Q.; Morokuma, K.; Bowman, J. M.; Klippenstein, S. J. *J. Chem. Phys.* **1999**, *110*, 9469–9482.
- (103) Grimme, S.; Woeller, M.; Peyerimhoff, S. D.; Danovich, D.; Shaik, S. *Chem. Phys. Lett.* **1998**, *287*, 601–607.
- (104) Harvey, J. N.; Grimme, S.; Woeller, M.; Peyerimhoff, S. D.; Danovich, D.; Shaik, S. *Chem. Phys. Lett.* **2000**, *322*, 358–362.
- (105) Note the possible size of nuclear quantum effects that will arise from H tunneling.
- (106) Zener, C. *Proc. R. Soc. London, A* **1932**, *137*, 696–702.
- (107) Zhu, C. Y.; Teranishi, Y.; Nakamura, H. In *Advanced Chemical Physics*; John Wiley & Sons Inc: New York, 2001; Vol. 117, pp 127–233.
- (108) Abramowitz, M.; Stegun, I. A. *Handbook of Mathematical Functions*; NBS: Washington, D.C., 1972; p 446.